



Cite this: *Chem. Commun.*, 2019, 55, 10916

Received 20th June 2019,  
Accepted 14th August 2019

DOI: 10.1039/c9cc04736k  
[rsc.li/chemcomm](http://rsc.li/chemcomm)

## Engineering dithiobenzoic acid lactone-decorated Si-rhodamine as a highly selective near-infrared HOCl fluorescent probe for imaging drug-induced acute nephrotoxicity†

Jinping Wang,‡ Dan Cheng,‡ Longmin Zhu, Peng Wang, Hong-Wen Liu, ID  
Mei Chen, ID\* Lin Yuan, ID and Xiao-Bing Zhang, ID\*

**A highly selective lysosome-targeting NIR fluorescent probe (Lyo-SiR-2S) for HOCl was constructed based on Si-rhodamine B spiro-dithiolactone. This probe was very effectively employed to sense HOCl produced in various living cells and to visualize fluctuations of endogenous HOCl resulting from GEN-induced acute kidney injury *in vivo* for the first time.**

Hypochlorous acid (HOCl) is a reactive oxygen species (ROS) that is generated for innate immunity by the peroxidation of chloride ion in the presence of myeloperoxidase (MPO).<sup>1</sup> It plays a vital role in preventing pathogen invasion and modulating cellular apoptosis.<sup>2</sup> However, aberrant generation of HOCl can cause oxidation of various biomolecules such as proteins and lipids, and further give rise to damage of cells and tissues.<sup>3</sup> As a result, excessive HOCl may lead to diseases related to inflammation and cancers.<sup>4</sup> Thus, it is imperative to develop effective tools for exploring subtle fluctuations of HOCl in living systems.

Fluorescence imaging features simplicity of operation, non-invasive detection, instantaneous response, and high sensitivity, and has thus been regarded as a powerful method to monitor substances in complex biosystems.<sup>5</sup> Fluorescence in the near-infrared range (NIR, 650–900 nm) is particularly suitable for application in biological imaging, owing to several attractive merits, such as low levels of photodamage, minimum interference from autofluorescence of the living organism, weak light scattering and deep tissue penetration. Many probes for HOCl based on naphthalimides,<sup>6</sup> rhodamine,<sup>7</sup> acedan,<sup>8</sup> or other fluorophores,<sup>9</sup> all displaying short emission wavelengths (<650 nm), have been developed (Table S1, ESI†). And a few NIR fluorescent probes for HOCl based on heptamethine cyanine dye (Cy7) or Si-rhodamine B were also reported.<sup>10</sup> Even so, further development of NIR fluorescent probes for HOCl is

still in demand. This demand is due in part to some NIR probes for HOCl such as Si-rhodamine B suffering to some extent from background signals, which would influence their ability to detect HOCl in practical applications. Moreover, these probes for HOCl often cannot distinguish HOCl from other ROSs or reactive nitrogen species (RNSs), especially  $\text{ONOO}^-$ .<sup>11</sup> It is thus a considerable challenge to improve the sensitivity and selectivity of the probes for HOCl.

The kidney organ normally performs the functions of clearing away endogenous waste substances in the body, metabolizing and eliminating xenobiotics such as administered drugs. As a result, the kidney is at risk for injury when exposed to high concentrations of drugs.<sup>12</sup> In fact, drug-induced renal injury is a common clinical dilemma, and many cases belong to the category of acute kidney injury (AKI). A possible mechanism involved here is the formation of ROSs and subsequent injurious oxidative stress. And HOCl may be produced during this process.<sup>13</sup> Generally, the direct nephrotoxic effects of ROSs are not only on mitochondria, leading to mitochondrial dysfunction and oxidative stress, but also on other subcellular organelles such as lysosomes. For example, gentamicin (GEN), an aminoglycoside drug, is taken in epithelial cells *via* endocytosis and mainly accumulates in lysosomes during acute nephrotoxicity, causing rupture of overloaded lysosomes. In this case, generation of ROSs including HOCl may occur in lysosomes.<sup>14</sup> However, to the best of our knowledge, no investigation of the potential of HOCl in lysosomes as an indicator for GEN-induced nephrotoxicity has yet been reported.

In view of these developments and remaining challenges, we set out to construct a robust lysosome-targeting NIR fluorescent probe possessing outstanding selectivity toward HOCl and low background fluorescence for visualizing HOCl changes *in vivo* during GEN-induced nephrotoxicity.

Si-Substituted rhodamine B not only keeps the superior qualities of the original rhodamine B such as adequate solubility in aqueous media and high quantum efficiency, but also demonstrates improved photostability and a long emission wavelength.<sup>15</sup> Si-Rhodamine B has therefore attracted considerable attention for

State Key Laboratory of Chemo/Biosensing and Chemometrics, College of Chemistry and Chemical Engineering, College of Materials Science and Engineering, Hunan University, Changsha, Hunan 410082, China. E-mail: [xbzhang@hnu.edu.cn](mailto:xbzhang@hnu.edu.cn), [chenmei@hnu.edu.cn](mailto:chenmei@hnu.edu.cn)

† Electronic supplementary information (ESI) available. See DOI: 10.1039/c9cc04736k

‡ These authors contributed equally to this work.

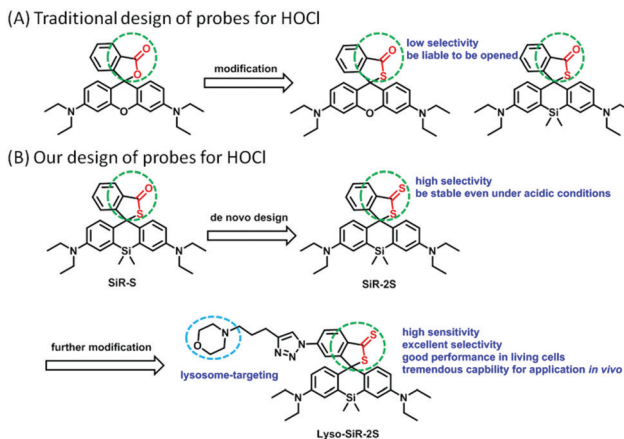


Fig. 1 The traditional design and our design of probes for HOCl based on (Si–) rhodamine B.

the design of NIR fluorescent probes for HOCl (Fig. 1A). However, the spiro ring formed by (thio)lactone generally tends to open even in the absence of target analyte, especially under acidic conditions (Fig. 1 and Fig. S2, ESI<sup>†</sup>). Consequently, these HOCl probes could exhibit some background fluorescence, leading to a low sensitivity for HOCl. Their application in imaging lysosomal HOCl is limited. Moreover, these probes are liable to sense both HOCl and  $\text{ONOO}^-$ , resulting in their poor selectivity. Therefore, we proposed that installing a dithiobenzoic acid lactone group on Si-rhodamine B rather than a thiobenzoic acid lactone would improve the selectivity and sensitivity of HOCl NIR probes. The gist for the design is that oxygen is more electronegative than sulfur and hence the carbon atom of a sulfur-substituted carbonyl ( $\text{C}=\text{S}$ ) is less electron-deficient than a normal carbonyl ( $\text{C}=\text{O}$ ). And indeed dithiobenzoic acid lactone was shown to be more stable than thiobenzoic acid lactone and to yield a lower background fluorescence and higher selectivity (Fig. S1, ESI<sup>†</sup>), in accordance with the reported higher reactivity of dithiobenzoic acid than of thiocarboxylic acid.<sup>16</sup> To verify our presumption, the compound **SiR-2S** was designed, and in the meantime the compound **SiR-S** was synthesized as a control compound for comparison (Fig. 1B).

We measured the spectral properties of **SiR-S** and **SiR-2S**. Since we expected Si-rhodamine B spirodithiolactones to be quite stable even under acidic conditions, these spectral measurements were performed at pH 4.5. The results confirmed that, compared to **SiR-S**, **SiR-2S** possessed lower background and better stability in the absence of HOCl, and higher selectivity (Fig. S2, ESI<sup>†</sup>). In addition, **SiR-2S** displayed more enhancement of fluorescence intensity after titration of the same amount of HOCl, which indicated a greater sensitivity of **SiR-2S** than of **SiR-S** to HOCl (Fig. S3, ESI<sup>†</sup>). Using the term  $3\sigma/k$ , **SiR-2S** was measured to display a detection limit for HOCl of 28 nM (Fig. S4, ESI<sup>†</sup>).

Subsequently, we studied the response mechanism. Rhodamine B thiolactone has been shown, upon encountering HOCl, to be converted to the corresponding ring-opened rhodamine B.<sup>17</sup> We envisaged that our probes **SiR-S** and **SiR-2S** after responding to HOCl would be transformed into the corresponding carboxylic

acids, due to the acidity and oxidation properties of HOCl. Indeed, the mass analysis for the mixture of **SiR-S** or **SiR-2S** and HOCl proved that assumption (Fig. S5, ESI<sup>†</sup>).

The results showed remarkable spectral properties displayed by the compound **SiR-2S** under acidic conditions, and indicated it to be an excellent candidate for constructing a lysosome-targeting probe for HOCl. Therefore, we incorporated a morpholine unit in **SiR-2S** through a click reaction of alkyne and azide to obtain **Lyso-SiR-2S** (Fig. 1B and Scheme S1, ESI<sup>†</sup>). Then its UV-vis spectrum and fluorescence as a function of the concentration of HOCl were examined. **Lyso-SiR-2S** displayed one gradually increasing broad absorption band centered at 667 nm after titration with HOCl (Fig. S6, ESI<sup>†</sup>). The maximum fluorescence emission peak was observed at 677 nm, and the intensity reached a plateau (83-fold enhancement) after addition of 60  $\mu\text{M}$  HOCl, accompanied by the mixture changing from colorless to watert blue in visible light (Fig. 2A and Fig. S7, ESI<sup>†</sup>).

The fluorescence intensity demonstrated an excellent linear relationship with HOCl concentration ( $R^2 = 0.993$ ) at low HOCl concentrations (0–1.0  $\mu\text{M}$ ) (Fig. S8, ESI<sup>†</sup>). After the calculation, almost the same detection limit of 25 nM was obtained here as was obtained for the only reported lysosome-targeting NIR probe for HOCl, *i.e.*, **Lyso-NIR-HOCl** (Table S1, ESI<sup>†</sup>). The high sensitivity of **Lyso-SiR-2S** was expected to enable it to track biogenic HOCl reliably. Its response mechanism was shown to be the same as that of the probe **SiR-2S** (Fig. S5, ESI<sup>†</sup>).

Then we also investigated the effects of various co-solvents and bovine serum albumin (BSA) on the response of the probe to HOCl to ensure its application *in vivo*. We found that the probe still displayed a good response either using different co-solvents or in the presence of BSA, and BSA did not quench the fluorescence of the response product (Fig. S9, ESI<sup>†</sup>). The results implied that the probe can be used for bioimaging *in vivo*. Afterwards we investigated the selectivity of **Lyso-SiR-2S** for HOCl over other relevant biological species, including ROSSs, RNSSs, RSSs, and metal ions. We observed a dramatic fluorescence intensity enhancement only after the probe reacted with HOCl, and there was no obvious change in fluorescence when **Lyso-SiR-2S** was exposed to other species (Fig. 2B). These results

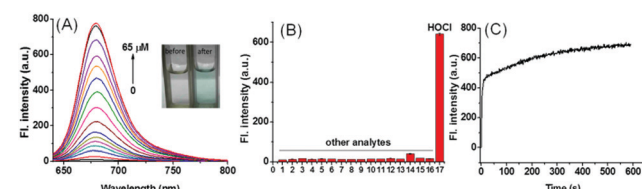


Fig. 2 (A) Fluorescence spectra of **Lyso-SiR-2S** (5  $\mu\text{M}$ ) in PBS (15% EtOH, pH 4.5) upon titration with HOCl,  $\lambda_{\text{ex}} = 616$  nm; inset: color change of the solution after the addition of HOCl under visible light. (B) The selective response of **Lyso-SiR-2S** (5  $\mu\text{M}$ ) toward various analytes (100  $\mu\text{M}$ , if not indicated): (1) blank; (2)–(8) in order:  $\text{Cu}^{2+}$ ;  $\text{Fe}^{3+}$ ;  $\text{Mg}^{2+}$ ;  $\text{Zn}^{2+}$ ;  $\text{Mn}^{2+}$ ;  $\text{K}^+$ ;  $\text{Na}^+$ ; (9)  $\text{Cys}$  (500  $\mu\text{M}$ ); (10)  $\text{H}_2\text{S}$ ; (11)–(16) in order:  $\text{H}_2\text{O}_2$ ;  $\text{O}_2\cdot^-$ ;  $t\text{-BuOOH}$ ;  $\text{ONOO}^-$ ;  $\text{HO}^\cdot$ ;  $t\text{-BuOO}^\cdot$ ; and (17) HOCl (50  $\mu\text{M}$ ). Each mixture was kept for 15 min at room temperature and then the fluorescence intensity was recorded. (C) Fluorescence of **Lyso-SiR-2S** (5  $\mu\text{M}$ ) at 677 nm as a function of time after the addition of 50  $\mu\text{M}$  HOCl.

indicated an excellent selectivity of **Lyso-SiR-2S** for HOCl. Afterwards, the fluorescence of **Lyso-SiR-2S** as a function of time after addition of 50  $\mu$ M HOCl was measured (Fig. 2C). The response here was almost finished within several seconds. Such a short response time is beneficial for real-time detection of endogenous HOCl fluctuation. Additionally, the fluorescence response of **Lyso-SiR-2S** to HOCl was also measured at various pH values (Fig. S10, ESI $\dagger$ ). The fluorescence intensity was observed to slightly decrease as the pH was increased from 4.0 to 9.0. It did not change too much over the lysosome pH range of 4.0–5.5. The results strongly suggested that it can work well as a lysosome-targeting probe.

Next, the probe **Lyso-SiR-2S** was used for fluorescence imaging in live cells. First, its biocompatibility was tested in HeLa cells by carrying out a standard MTT assay (Fig. S11, ESI $\dagger$ ). This test disclosed a low cytotoxicity of the probe. Then we used one-photon microscopy imaging to examine the ability of **Lyso-SiR-2S** to respond to exogenous HOCl in live HeLa cells and endogenous HOCl in RAW264.7 macrophages (Fig. S12 and S13, ESI $\dagger$ ). The results indicated that **Lyso-SiR-2S** can be effectively used to monitor the fluctuations in the concentration of HOCl in live cells.

Inspired by the prominent detection ability of **Lyso-SiR-2S**, we further tried to explore its potential biological application to visualize HOCl in live human kidney 2 (HK-2) cells with GEN-induced nephrotoxicity. We measured the fluorescence of **Lyso-SiR-2S** as a function of cell incubation time with GEN (3 mM) in HK-2 cells. The cells incubated with the probe for only 1 h showed negligible fluorescence (Fig. S14, ESI $\dagger$ ). Those pretreated with GEN for 4 h exhibited weak fluorescence, and a remarkable enhancement was observed after incubation for 8 h or 12 h. Thus 8 h was chosen as the incubation time for the following study. For the probe, the response in fact was observed to be completed within about 30 min (Fig. S15, ESI $\dagger$ ), and incubation for 90 min did not cause cell death, in contrast with Lyso-Tracker Red (Fig. S16, ESI $\dagger$ ).<sup>18</sup> Here we incubated cells with the probe for 1 h. L-Carnitine (LC) as an antioxidant was reported to have a renoprotective effect in some drug-induced nephrotoxicity cases such as those caused by cisplatin, doxorubicin, and CsA.<sup>19</sup> So we then measured fluorescence levels with various concentrations of GEN and LC. As shown in Fig. 3, the fluorescence intensity increased as the HK-2 cells were pretreated with an increasing concentration of GEN from 1 to 3 to 6 mM, but decreased when LC (1 or 3 mM) was also included. Overall, the results showed that **Lyso-SiR-2S** can detect HOCl generated as a result of GEN-induced nephrotoxicity at the cellular level and that LC can reduce the amount of HOCl and hence provide renoprotection during this process.

As previously mentioned, GEN mainly accumulates in lysosomes, where HOCl may be produced. To evaluate the subcellular target specificity of **Lyso-SiR-2S**, colocalization experiments were performed in HK-2 cells. As seen in Fig. S17 (ESI $\dagger$ ), the fluorescence of the probe overlapped well with that of Lyso-Tracker Green, but not with that of Mito-Tracker Red, yielding Pearson's correlation coefficients of 0.81 and 0.52, respectively. Furthermore, we confirmed that the probe can target lysosomes

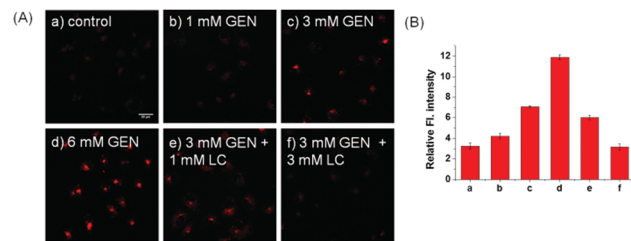


Fig. 3 (A) Confocal fluorescence images of HK-2 cells. The concentration of our probe was 10  $\mu$ M. (a) Cells were incubated with probe; (b–d) cells were cocultured in advance with GEN (1, 3, or 6 mM) for 8 h, then with the probe for 1 h; (e and f) cells were cocultured in advance with GEN (3 mM) and LC (1 or 3 mM) for 8 h, then the probe for 1 h.  $\lambda_{\text{ex}} = 635$  nm,  $\lambda_{\text{em}} = 650$ –750 nm. (B) Average values of the corresponding fluorescence intensities from the images in (A). Scale bar: 20  $\mu$ m.

in HeLa cells and RAW264.7 macrophages (Fig. S18, ESI $\dagger$ ), showing Pearson's correlation coefficients of 0.83 and 0.84 respectively. We thus concluded that the probe can specifically localize and detect endogenous HOCl in subcellular organelles, in contrast with compound **SiR-2S** (Fig. S19, ESI $\dagger$ ).

The strong fluorescence of the probe **Lyso-SiR-2S** in HK-2 cells with GEN-induced injury verified the theoretical speculation that HOCl is one kind of ROS generated during nephrotoxicity events. Therefore, we further investigated the capability of the probe to monitor endogenous HOCl produced *in vivo* during GEN-induced nephrotoxicity. When the tested mice were pre-injected with GEN or PBS and then injected with **Lyso-SiR-2S**, the former showed stronger fluorescence than did the latter. Meanwhile, we did not observe any fluorescence signal in the kidneys of intact mice (Fig. 4A). Various doses of

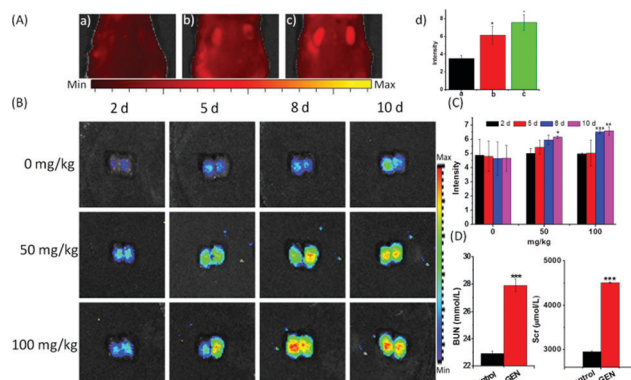


Fig. 4 (A) Fluorescence imaging of mice *in vivo* with GEN-induced nephrotoxicity. (a) Images of intact mice, and (b and c) mice injected with PBS (b) or GEN (50  $\text{mg kg}^{-1}$ ) (c) into the abdominal cavity for 8 d, and then intravenously injected with **Lyso-SiR-2S** in PBS (100  $\mu\text{L}$ , 200  $\mu\text{M}$ ). (d) Average values of corresponding fluorescence intensities from the images in a–c. (B) Renal fluorescence images of mice. The mice were pretreated with GEN at different doses (0, 50, 100  $\text{mg kg}^{-1}$ ) for different injection times (2, 5, 8, 10 d), and then treated with the probe (100  $\mu\text{L}$ , 100  $\mu\text{M}$ ) for 3 h. Then the dissected kidneys were used for imaging ( $\lambda_{\text{ex}} = 640$  nm,  $\lambda_{\text{em}} = 695$ –770 nm). (C) Average values of fluorescence intensity corresponding to the images in (B). (D) Concentrations of blood urea (BUN) and serum creatinine (Scr) in the control and GEN (100  $\text{mg kg}^{-1}$ ) groups. The values displayed are mean values  $\pm$  SD,  $n = 3$ , \* $p < 0.05$ , \*\* $p < 0.01$ , \*\*\* $p < 0.001$ .

GEN (0, 50, 100 mg kg<sup>-1</sup>) were also administered through intra-peritoneal injection for various durations (2, 5, 8, 10 d). Afterwards, the solution of the **Lyso-SiR-2S** probe in PBS was injected *via* the tail vein. Fluorescence imaging of the harvested kidneys was performed after 3 h. As shown in Fig. 4B and C, when the mice were not treated with GEN, the fluorescence of the kidneys hardly changed (the other images for the control are shown in Fig. S20, ESI†). In contrast, an obvious enhancement of the signal was observed post GEN injection. And comparisons of the duration of 2 d with other durations at the same dose of GEN showed the dose of 100 mg kg<sup>-1</sup> for 8 d leading to relatively severe nephrotoxicity. In the meantime, we also measured the concentrations of blood urea and serum creatinine, which are conventional bio-markers of acute kidney injury.<sup>20</sup> As displayed in Fig. 4D, the mice subjected to a GEN (100 mg kg<sup>-1</sup>) injection for 8 d showed higher serum creatinine and blood urea concentrations than did the control group. GEN was concluded to have caused severe kidney injury. The results indicated an up-regulation of the level of HOCl in the mice suffering from GEN-induced kidney failure. Our **Lyso-SiR-2S** probe was apparently able to detect GEN-induced nephrotoxicity *in vivo* by reacting with endogenous HOCl generated during this process, demonstrating its potential application in the diagnosis and pathological study of GEN-induced nephrotoxicity.

In summary, we first designed a highly sensitive **SiR-2S** probe by employing a dithiobenzoic acid lactone recognition unit instead of thiobenzoic acid lactone, and successfully improved the selectivity of the Si-rhodamine B thiolactone probe (**SiR-S**) for HOCl. The **SiR-2S** probe also showed good stability, even under acidic conditions. Thus we further developed a lysosome-targeting NIR fluorescent probe, **Lyso-SiR-2S**, with low levels of background signals. It presented a detection limit of 25 nM and a fast response, within several seconds. What is more, **Lyso-SiR-2S** retained excellent selectivity for HOCl over other ROSS and RNSs. These features enable it to directly detect fluctuations of exogenous and endogenous HOCl in living HeLa and RAW264.7 cells. In addition, the good performance of **Lyso-SiR-2S** for fluorescence imaging implied that it can capture endogenous HOCl generated in live HK-2 cells and in kidneys of mice *in vivo* during GEN-induced acute renal injury, and such a detection was here achieved for the first time. This probe is promising as a powerful and convenient imaging tool for the diagnosis and pathophysiological study of drug-induced acute nephrotoxicity.

The work was supported by the NSFC (21890744, 21877029, 21622504, 21705037), the Science and Technology Project of Hunan Province (2017RS3019) and the China Postdoctoral Science Foundation (2018M642968).

## Conflicts of interest

There are no conflicts to declare.

## Notes and references

1 S. J. Klebanoff, *J. Leukocyte Biol.*, 2005, **77**, 598.

2 (a) C. C. Winterbourn, M. B. Hampton, J. H. Livesey and A. J. Kettle, *J. Biol. Chem.*, 2006, **281**, 39860; (b) M. Whiteman, P. Rose, J. L. Siau, N. S. Cheung, G. S. Tan, B. Halliwell and J. S. Armstrong, *Free Radical*

*Biol. Med.*, 2005, **38**, 1571; (c) D. I. Pattison and M. J. Davies, *Curr. Med. Chem.*, 2006, **13**, 3271; (d) C. Gorrini, I. S. Harris and T. W. Mak, *Nat. Rev. Drug Discovery*, 2013, **12**, 931; (e) T. Strowig, J. Henao-Mejia, E. Elinav and R. Flavell, *Nature*, 2012, **481**, 278.

3 J. Winter, M. Ilbert, P. C. Graf, D. Ozcelik and U. Jakob, *Cell*, 2008, **135**, 691.

4 (a) L. J. Hazell, L. Arnold, D. Flowers, G. Waeg, E. Malle and R. Stocker, *J. Clin. Invest.*, 1996, **97**, 1535; (b) R. P. Wu, T. Hayashi, H. B. Cottam, G. Jin, S. Yao, C. C. Wu, M. D. Rosenbach, M. Corr, R. B. Schwab and D. A. Carson, *Proc. Natl. Acad. Sci. U. S. A.*, 2010, **107**, 7479.

5 (a) Y. Lv, D. Cheng, D. Su, M. Chen, B.-C. Yin, L. Yuan and X.-B. Zhang, *Chem. Sci.*, 2018, **9**, 7606; (b) D. Cheng, J. Peng, Y. Lv, D. Su, D. Liu, M. Chen, L. Yuan and X.-B. Zhang, *J. Am. Chem. Soc.*, 2019, **141**, 6352; (c) J. Huang, J. Li, Y. Lyu, Q. Miao and K. Pu, *Nat. Mater.*, 2019, DOI: 10.1038/s41563-019-0378-4; (d) D. Cheng, W. Xu, L. Yuan and X.-B. Zhang, *Anal. Chem.*, 2017, **89**, 7693; (e) X. Jia, Q. Chen, Y. Yang, Y. Tang, R. Wang, Y. Xu, W. Zhu and X. Qian, *J. Am. Chem. Soc.*, 2016, **138**, 10778.

6 (a) Q. Duan, P. Jia, Z. Zhuang, C. Liu, X. Zhang, Z. Wang, W. Sheng, Z. Li, H. Zhu, B. Zhu and X. Zhang, *Anal. Chem.*, 2019, **91**, 2163; (b) P. Zhang, H. Wang, Y. Hong, M. Yu, R. Zeng, Y. Long and J. Chen, *Biosens. Bioelectron.*, 2018, **99**, 318; (c) H. Feng, Z. Zhang, Q. Meng, H. Jia, Y. Wang and R. Zhang, *Adv. Sci.*, 2018, **5**, 1800397.

7 (a) C. Zhang, Q. Nie, I. Ismail, Z. Xi and L. Yi, *Chem. Commun.*, 2018, **54**, 3835; (b) X. Jiao, Y. Xiao, Y. Li, M. Liang, X. Xie, X. Wang and B. Tang, *Anal. Chem.*, 2018, **90**, 7510.

8 (a) Z. Mao, M. Ye, W. Hu, X. Ye, Y. Wang, H. Zhang, C. Li and Z. Liu, *Chem. Sci.*, 2018, **9**, 6035; (b) L. Yuan, L. Wang, B. K. Agrawalla, S. J. Park, H. Zhu, B. Sivaraman, J. Peng, Q. H. Xu and Y. T. Chang, *J. Am. Chem. Soc.*, 2015, **137**, 5930.

9 (a) Y. L. Pak, S. J. Park, D. Wu, B. Cheon, H. M. Kim, J. Bouffard and J. Yoon, *Angew. Chem., Int. Ed.*, 2018, **57**, 1567; (b) L. Wu, I. C. Wu, C. C. DuFort, M. A. Carlson, X. Wu, L. Chen, C.-T. Kuo, Y. Qin, J. Yu, S. R. Hingorani and D. T. Chiu, *J. Am. Chem. Soc.*, 2017, **139**, 6911; (c) H. Zhu, J. Fan, J. Wang, H. Mu and X. Peng, *J. Am. Chem. Soc.*, 2014, **136**, 12820; (d) Y.-X. Liao, M.-D. Wang, K. Li, Z.-X. Yang, J.-T. Hou, M.-Y. Wu, Y.-H. Liu and X.-Q. Yu, *RSC Adv.*, 2015, **5**, 18275; (e) X. Xie, T. Wu, X. Wang, Y. Li, K. Wang, Z. Zhao, X. Jiao and B. Tang, *Chem. Commun.*, 2018, **54**, 11965.

10 (a) H. Li, L. Guan, X. Zhang, H. Yu, D. Huang, M. Sun and S. Wang, *Talanta*, 2016, **161**, 592; (b) L.-L. Xi, X.-F. Guo, C.-L. Wang, W.-L. Wu, M.-F. Huang, J.-Y. Miao and B.-X. Zhao, *Sens. Actuators, B*, 2018, **255**, 666; (c) P. Wei, L. Liu, Y. Wen, G. Zhao, F. Xue, W. Yuan, R. Li, Y. Zhong, M. Zhang and T. Yi, *Angew. Chem., Int. Ed.*, 2019, **58**, 4547; (d) Y. Koide, Y. Urano, K. Hanaoka, T. Terai and T. Nagano, *J. Am. Chem. Soc.*, 2011, **133**, 5680; (e) G.-J. Mao, Z.-Z. Liang, J. Bi, H. Zhang, H.-M. Meng, L. Su, Y.-J. Gong, S. Feng and G. Zhang, *Anal. Chim. Acta*, 2019, **1048**, 143; (f) P. Wei, W. Yuan, F. Xue, W. Zhou, R. Li, D. Zhang and T. Yi, *Chem. Sci.*, 2018, **9**, 495.

11 H. Zhang, J. Liu, C. Liu, P. Yu, M. Sun, X. Yan, J. P. Guo and W. Guo, *Biomaterials*, 2017, **133**, 60.

12 K. Hosohata, *Int. J. Mol. Sci.*, 2016, **17**, 1826.

13 P. D. Walker, Y. Barri and S. V. Shah, *Renal Failure*, 1999, **21**, 433.

14 (a) Y. I. Mahmoud, *Biomed. Pharmacother.*, 2017, **94**, 206; (b) H.-S. Shin, M. Yu, M. Kim, H. S. Choi and D.-H. Kang, *Lab. Invest.*, 2014, **94**, 1147.

15 (a) Y. Koide, Y. Urano, K. Hanaoka, T. Terai and T. Nagano, *ACS Chem. Biol.*, 2011, **6**, 600; (b) T. E. McCann, N. Kosaka, Y. Koide, M. Mitsunaga, P. L. Choyke, T. Nagano, Y. Urano and H. Kobayashi, *Bioconjugate Chem.*, 2011, **22**, 2531.

16 O. Bettucci, D. Franchi, A. Sinicropi, M. di Donato, P. Foggi, F. Fabrizi de Biani, G. Reginato, L. Zani, M. Calamante and A. Mordini, *Eur. J. Org. Chem.*, 2019, 812.

17 X.-Q. Zhan, J.-H. Yan, J.-H. Su, Y.-C. Wang, J. He, S.-Y. Wang, H. Zheng and J.-G. Xu, *Sens. Actuators, B*, 2010, **150**, 774.

18 C. S. Abeywickrama, K. J. Wijesinghe, R. V. Stahelin and Y. Pang, *Chem. Commun.*, 2019, **55**, 3469.

19 (a) Y. Liu, S. Yan, C. Ji, W. Dai, W. Hu, W. Zhang and C. Mei, *Kidney Blood Pressure Res.*, 2012, **35**, 373; (b) N. Origlia, M. Migliori, V. Panichi, C. Filippi, A. Bertelli, A. Carpi and L. Giovannini, *Biomed. Pharmacother.*, 2006, **60**, 77.

20 J. H. Cheon, S. Y. Kim, J. Y. Son, Y. R. Kang, J. H. An, J. H. Kwon, H. S. Song, A. Moon, B. M. Lee and H. S. Kim, *Toxicol. Res.*, 2016, **32**, 47.